

Strain and origin of inhomogeneous broadening probed by optically detected nuclear magnetic resonance in a (110) GaAs quantum well

M. Ono, J. Ishihara, G. Sato, S. Matsuzaka, Y. Ohno,^{*,†} and H. Ohno

Laboratory for Nanoelectronics and Spintronics, Research Institute of Electrical Communication,
Tohoku University, Katahira 2-1-1, Aoba-ku, Sendai 980-8577, Japan

(Received 21 August 2012; revised manuscript received 23 June 2013; published 11 March 2014)

We obtained strain and electric field gradient (EFG) in an n -GaAs/Al_{0.3}Ga_{0.7}As (110) quantum well (QW) by optically detected nuclear magnetic resonance (NMR). The dependence of the quadrupolar splitting on an angle between the QW plane and a static magnetic field provided the crystalline-orientation-dependent EFG and strain in the GaAs QW. We also explored the dependence of the NMR line widths on the direction of the external magnetic field with respect to the QW plane. It is likely that the nonuniform EFG as well as the hyperfine interaction governs the inhomogeneous broadening of NMR spectra.

DOI: [10.1103/PhysRevB.89.115308](https://doi.org/10.1103/PhysRevB.89.115308)

PACS number(s): 85.75.-d, 76.60.-k, 76.70.Hb, 78.66.Fd

Degrees of symmetry of potential and internal electric field are of importance for electron and nuclear spin states in semiconductors. Strain inside semiconductors plays a key role for nuclear spin dynamics because it reduces the structural symmetry. In GaAs-based systems, the quadrupole interaction is enhanced by breaking symmetry of the electric field gradient (EFG) [1], which depends on the applied static magnetic field [2]. It is well known that the EFG is induced by strain [3], and the relation between strain and the EFG has been studied in bulk GaAs [4,5]. Recently, the quadrupolar splitting has been highlighted to examine mechanically controlled strain [6,7] and mapping of the strain distribution [8] in quantum wells (QWs). The investigation of the quadrupole interaction can provide rich information about internal electronic states as well as nuclear spin dynamics [9–12].

In this work, we quantitatively studied unintentional strain in GaAs/AlGaAs QWs by evaluating the EFG. The quadrupole interaction is dependent not only on the amplitude of the EFG but also the angle between the static magnetic field and the principal axes of the EFG [13]. In this letter, we analyzed the dependence of the quadrupolar splitting on these parameters in a strained n -(110) GaAs QW, detected by optical time-resolved Faraday rotation (TRFR) technique. The angle dependence of the nuclear magnetic resonance (NMR) line widths is also discussed.

In the experiments, we used a single QW sample grown on a (110) GaAs substrate by molecular beam epitaxy. It consists of, from the top of the epilayers, a 5-nm GaAs cap layer, a 500-nm-thick Al_{0.3}Ga_{0.7}As top barrier, an 8.5-nm-thick n -GaAs QW with Si donors doped at $5 \times 10^{17} \text{ cm}^{-3}$, a 500-nm-thick Al_{0.3}Ga_{0.7}As bottom barrier, and a GaAs buffer layer. The growth temperature was around 480 °C, and GaAs growth rate was 0.7 $\mu\text{m/h}$. For optical transmission measurements, the epilayer was glued on a fused silica glass with epoxy, and the GaAs buffer and substrate were removed by selective chemical etching. Thus the remaining 500+500 nm Al_{0.3}Ga_{0.7}As sandwiching the 8.5-nm GaAs QW is expected to be relaxed to its own lattice constant

after removing the GaAs substrate. The sample was set in a cryostat with a superconducting magnet, which generates a static magnetic field \mathbf{B}_0 , and a Helmholtz coil for applying a rf magnetic field $\mathbf{B}_{\text{rf}}(\omega t)$. In our experimental configuration, the coordinate is taken so that the directions of the optical path// x , $\mathbf{B}_{\text{rf}}(\omega t)$ // y and \mathbf{B}_0 // z cross each other at right angles, as shown in Fig. 1(a). The sample can be rotated by an angle α with respect to \mathbf{B}_0 and an angle β about the [110] crystalline orientation, respectively. The position at $\alpha = \beta = 0^\circ$ are taken so that \mathbf{B}_0 //[001] and $\mathbf{B}_{\text{rf}}(\omega t)$ // $[\bar{1}10]$. For optical detection of NMR, we used the TRFR technique in which the nuclear magnetic field \mathbf{B}_n is detected by the change of the phase of the photoexcited electron spin precession [14–18]. We set the power of circular-polarized pump and linear-polarized probe beams at 8 mW and 0.4 mW. The diameter of the laser spot size was $\sim 30 \mu\text{m}$ on the sample. Figure 1(b) shows a typical TRFR-detected NMR spectrum of ^{75}As obtained at $T = 4.6 \text{ K}$, $B_0 = 1.0 \text{ T}$, $\alpha = -5^\circ$, and $\beta = 0^\circ$. We chose $\alpha = -5^\circ$ to enhance the dynamic nuclear polarization (DNP), which is induced by the contact hyperfine interaction and gives better signal to noise ratio. The data was taken by measuring the Faraday rotation angle θ_F with changing the rf frequency ω of \mathbf{B}_{rf} . The sweep rate of ω was 0.2 kHz/s. The asymmetric line shape is due to the long nuclear spin relaxation time (a few minutes) compared to the ω sweep rate.

In GaAs QW, there are three species of nuclei that have $I = 3/2$: ^{75}As , ^{71}Ga , and ^{69}Ga . When \mathbf{B}_0 is applied, the nuclear spin states separate into four levels. In the presence of the noncentrosymmetric EFG, the quadrupole interaction makes an energy separation between two neighboring levels, $|m\rangle$ and $|m-1\rangle$ ($m = 3/2, 1/2, \text{ and } -1/2$), different from each other, as shown by the inset of Fig. 1(b). Then the nuclear spin states are described on the basis of $|m\rangle$ by the following Hamiltonian,

$$\hat{H} = -\gamma \hbar \mathbf{B}_0 \cdot \mathbf{I} + \frac{eQ}{12} \times \begin{pmatrix} \sqrt{6}V_{2,0} & 2\sqrt{3}V_{2,-1} & 2\sqrt{3}V_{2,-2} & 0 \\ -2\sqrt{3}V_{2,1} & -\sqrt{6}V_{2,0} & 0 & 2\sqrt{3}V_{2,-2} \\ 2\sqrt{3}V_{2,2} & 0 & -\sqrt{6}V_{2,0} & -2\sqrt{3}V_{2,-1} \\ 0 & 2\sqrt{3}V_{2,2} & 2\sqrt{3}V_{2,1} & \sqrt{6}V_{2,0} \end{pmatrix}, \quad (1)$$

*Corresponding author: oono@bk.tsukuba.ac.jp

†Present address: Faculty of Pure and Applied Sciences, University of Tsukuba, Tsukuba Japan.

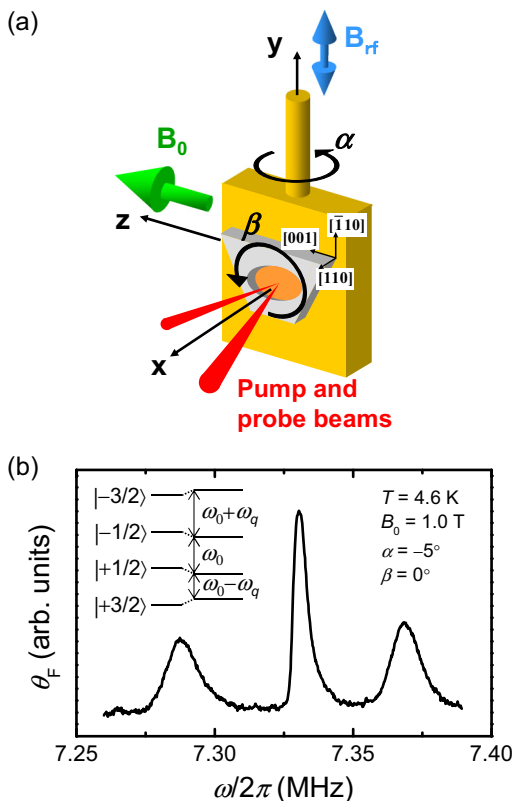


FIG. 1. (Color online) (a) Schematic of the measurement geometry. The sample was rotated by angles α and β around \mathbf{B}_{rf} and the [110] crystalline orientation of the sample, respectively. At $\alpha = \beta = 0^\circ$, the [110], $[\bar{1}10]$, and [001] axes of the sample were along the directions of the incident laser beams, \mathbf{B}_{rf} and \mathbf{B}_0 , respectively. (b) TRFR-detected NMR spectrum of ^{75}As at $T = 4.6$ K, $B_0 = 1.0$ T, $\alpha = -5^\circ$, and $\beta = 0^\circ$. The inset is the energy diagram of the quadrupolar-split nuclear spin states.

where γ is the nuclear gyromagnetic ratio, \hbar is the reduced Planck constant, e is the elementary electric charge, and Q is the quadrupole moment. $V_{2,0} = 3V_{zz}/\sqrt{6}$, $V_{2,\pm 1} = \mp(V_{zx} \pm iV_{zy})$, and $V_{2,\pm 2} = (V_{xx} - V_{yy})/2 \pm iV_{xy}$ are the spherical tensor coefficients, and $V_{ij} = \partial^2 V / \partial i \partial j$ ($i, j = x, y, z$) are the components of the EFG [1]. The first term in Eq. (1) is the Zeeman term, and the second term corresponds to the quadrupolar splitting on the basis of $|m\rangle$. V_{ij} is expressed by the coordinate transformation of the EFG corresponding to the crystalline orientation $V'_{kl} = \partial^2 V / \partial k \partial l$ ($k, l = X/[100], Y/[010], Z/[001]$) [19], which is given by the product of the elastic strain tensor $\boldsymbol{\varepsilon}$ and the fourth order tensor \mathbf{S} , which connects the EFG tensor at the nucleus with the strain deformation tensor [3] as

$$V'_{kl} = \sum_{m,n} S_{klmn} \varepsilon_{mn} (k, l, m, n = X, Y, Z). \quad (2)$$

Suppose that only an in-plane stress exists in this (110) QW sample, $\varepsilon_{XX} = \varepsilon_{YY}$ and $\varepsilon_{ZX} = \varepsilon_{ZY}$. In the Voigt notation, Eq. (2) gives

$$\begin{aligned} V'_{ZZ} &= -2V'_{XX} = -2V'_{YY} = S_{11}(\varepsilon_{ZZ} - \varepsilon_{XX}), \\ V'_{XY} &= 2S_{44}\varepsilon_{XY}, \end{aligned} \quad (3)$$

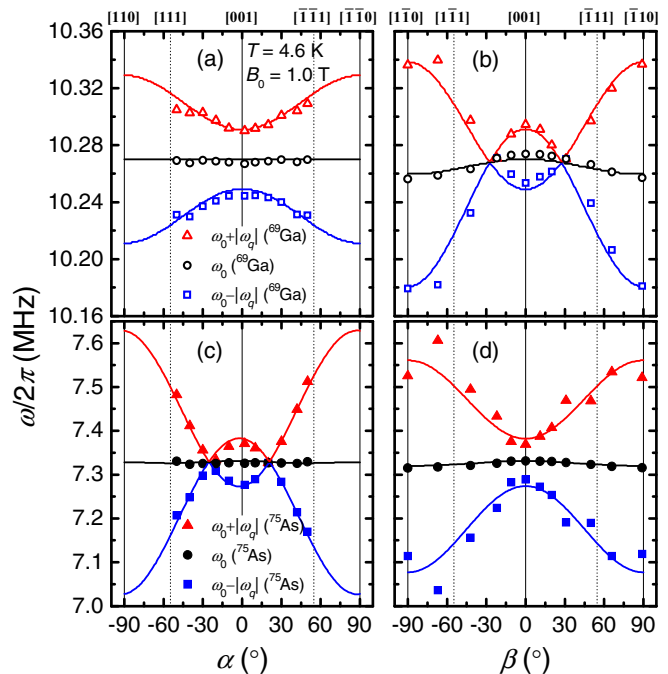


FIG. 2. (Color online) α dependence of the resonance frequencies of ^{69}Ga (a) and ^{75}As (c). β dependence of those of ^{69}Ga (b) and ^{75}As (d). The α dependence was measured at $\beta = 0^\circ$, and the β dependence was measured at $\alpha = -5^\circ$. The upper label indicates the crystalline orientation corresponding to each angle (there is displacement by -5° in β dependence).

$$V'_{ZX} = V'_{ZY} = 2S_{44}\varepsilon_{ZX}.$$

An analytic expression of the quadrupolar splitting $\hbar\omega_q$ is given by

$$\begin{aligned} \hbar\omega_q &= \frac{eQ}{2} \left\{ \frac{3\cos^2\alpha\cos^2\beta - 1}{2} V'_{ZZ} \right. \\ &\quad + (\sin^2\alpha - \cos^2\alpha\sin^2\beta) V'_{XY} \\ &\quad \left. - \sqrt{2}\sin 2\alpha\cos\beta V'_{ZX} \right\}. \end{aligned} \quad (4)$$

We first investigated the α and β dependence of the NMR spectra of ^{75}As and ^{69}Ga measured at $T = 4.6$ K and $B_0 = 1$ T. The resonance frequencies were obtained by Gaussian fitting of the optically detected NMR spectra, provided that there exists time-independent fluctuation such as nonuniform EFG [1]. The results are shown by symbols in Figs. 2(a) and 2(b) for ^{75}As and in Figs. 2(c) and 2(d) for ^{69}Ga . The data in Figs. 2(a) and 2(c) were taken at $-50^\circ < \alpha < 50^\circ$ and at $\beta = 0^\circ$, and those in Figs. 2(b) and 2(d) were taken at $-90^\circ < \beta < 90^\circ$ and $\alpha = -5^\circ$. Three resonance frequencies correspond to the transition energies of $\omega_0 + |\omega_q|$, ω_0 , and $\omega_0 - |\omega_q|$, where $\hbar\omega_0$ and $\hbar\omega_q$ are the Zeeman and the quadrupolar splitting energies. We calculated the α and β dependence of the resonance frequency from Eq. (1), whose parameters were optimized by fitting [20]. The results are shown in Figs. 2(a)–2(d) by solid curves. The EFG values obtained by the fitting are (in units of 10^{19} V/m 2) as follows: $V'_{ZZ} = \pm 1.6$, $V'_{XY} = \mp 7.8$, and $V'_{ZX} = \pm 0.3$ for ^{75}As ; $V'_{ZZ} = \pm 0.9$, $V'_{XY} = \pm 3.0$, and $V'_{ZX} = 0.0$ for ^{69}Ga [21]. Based on these EFG values, we

evaluate strain in the QW from Eq. (3). S_{11} and S_{44} are determined by the nuclear acoustic resonance measurement (in units of 10^{15} statcoulomb/cm³) and are taken from the literature [4]: $S_{11} = \pm 13.2$ and $S_{44} = \pm 26.5$ for ⁷⁵As and $S_{11} = \mp 9.1$ and $S_{44} = \pm 9.2$ for ⁶⁹Ga, respectively. The obtained parameters for strain are $|\varepsilon_{ZZ} - \varepsilon_{XX}| = 3.9 \times 10^{-4}$, $|\varepsilon_{XY}| = 4.9 \times 10^{-4}$, and $|\varepsilon_{ZX}| = 0.2 \times 10^{-4}$ for ⁷⁵As and $|\varepsilon_{ZZ} - \varepsilon_{XX}| = 3.3 \times 10^{-4}$, $|\varepsilon_{XY}| = 5.5 \times 10^{-4}$, and $|\varepsilon_{ZX}| = 0.0 \times 10^{-4}$ for ⁶⁹Ga. These evaluated for ⁷⁵As and ⁶⁹Ga are almost the same as each other, which supports that we obtained the EFG correctly. Assuming that the in-plane lattice constant of GaAs becomes equal to that of Al_{0.3}Ga_{0.7}As, the in-plane strain is to be $\varepsilon_{//} = 4.1 \times 10^{-4}$ [22]. In the (X , Y , Z) coordinate, the components of ε are given by

$$\begin{aligned} \varepsilon_{XX} = \varepsilon_{YY} &= -\frac{C_{12} - 2C_{44}}{C_{11} + C_{12} + 2C_{44}}\varepsilon_{//}, & \varepsilon_{ZZ} &= \varepsilon_{//}, \\ \varepsilon_{XY} &= -\frac{C_{11} + 2C_{12}}{C_{11} + C_{12} + 2C_{44}}\varepsilon_{//}, & \varepsilon_{YZ} = \varepsilon_{XZ} &= 0, \end{aligned} \quad (5)$$

where C_{11} , C_{12} , and C_{44} are the elastic stiffness constants [23]. Using the GaAs parameters of $C_{11} = 11.88$, $C_{12} = 5.38$, and $C_{44} = 5.94$ (in units of 10^{11} dyne/cm²) [24], we obtain $\varepsilon_{XX} - \varepsilon_{ZZ} = \varepsilon_{XY} = -3.2 \times 10^{-4}$. The experimentally evaluated strain has the same order of that induced by the lattice mismatch between GaAs and Al_{0.3}Ga_{0.7}As. As for the discrepancy, it might be owing to the difference of the coefficients of the thermal expansion between the epoxy and GaAs, which causes the comparable strain in a GaAs QW [25–27]. Therefore, it might be that the present QW sample strain was induced mainly by the lattice mismatch and additionally by the thermal stress by the epoxy.

Finally, we discuss the α and β dependence of the line widths of the NMR spectra. Figure 3 shows (a) α and (b) β dependence of the line widths (full width at half maximum [FWHM]) for $\omega = \omega_0$ and $\omega = \omega_0 - |\omega_q|$ resonance peaks of ⁷⁵As and ⁶⁹Ga. When $|\alpha|$ is increased (β is fixed at 0°), both line widths of $\omega = \omega_0$ and $\omega_0 - |\omega_q|$ become broader, as shown in Fig. 3(a). In Fig. 3(b), on the other hand, the line width of the ω_0 resonance peak is almost constant, while that of the $\omega_0 - |\omega_q|$ resonance peak increases drastically with β (α is fixed at -5°).

Now we consider these observations by taking into account the DNP and the quadrupole interaction. First, we examined the α and β dependence of the DNP. The α and β dependence of the degree of nuclear polarization along the external magnetic field was examined by measuring the Larmor precession frequency ν_L of electron spins as functions of α and β , which are shown by symbols in Figs. 3(c) and 3(d). The solid curves are the α and β dependence of ν_L without \mathbf{B}_n that is calculated by taking into account the anisotropic electron \mathbf{g} tensor. The degree of nuclear spin polarization is about 7% at $\alpha = -5^\circ$ and $\beta = 0^\circ$. As shown in Fig. 3(c), ν_L increases significantly by increasing $|\alpha|$ as a consequence that the time-averaged electron spins increases with increasing $|\alpha|$; thus, DNP is enhanced [15]. With changing β , on the other hand, ν_L is almost constant since the time-averaged electron spin does not change with β [as shown in Fig. 3(d)]. This can qualitatively explain the increase of the line widths with $|\alpha|$, shown in Fig. 3(a). While efficient DNP by optical orientation is desired to achieve high

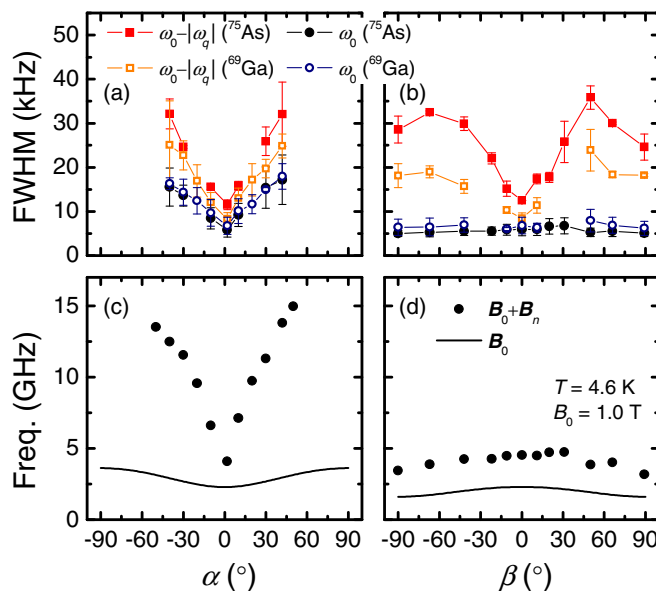


FIG. 3. (Color online) (a) α and (b) β dependence of the line widths of ⁶⁹Ga and ⁷⁵As at $T = 4.6$ K, $B_0 = 1.0$ T. The α dependence was measured at $\beta = 0^\circ$, and the β dependence was measured at $\alpha = -5^\circ$. (c) α and (d) β dependence of the Larmor frequency of the photoexcited electron spins at $T = 4.6$ K, $B_0 = 1.0$ T. We also plot the frequency without \mathbf{B}_n obtained from the calculation. The g factors $|g_{110}| = 0.26$, $|g_{\bar{1}\bar{1}0}| = 0.11$, and $|g_{001}| = 0.16$ were obtained from the Larmor frequency of the electron spins measured with the photoelastic modulator to avoid dynamic nuclear polarization.

nuclear spin polarization states, this increase of the effective and random magnetic field by the electron spins (not parallel to the \mathbf{B}_0 because of anisotropic \mathbf{g} tensor) should result in the enhancement of the precession of nuclear spins, which tends to align along \mathbf{B}_0 [28], and may lead to the fast dephasing of the ensemble nuclear spins. This qualitatively explains why all the resonance line widths become broader as $|\alpha|$ is increased from zero.

Next, we consider the effect of the quadrupolar interaction. Based on the first-order perturbation theory, Eq. (1) gives the energy separation between two neighboring states as

$$E_m - E_{m-1} = -\gamma \hbar B_0 + \frac{eQV_{ZZ}}{2} \left(m - \frac{1}{2} \right). \quad (6)$$

This reveals that the NMR peaks become broad for $\omega = \omega_0 \pm \omega_q$ resonance if the EFG (V'_{XX} , V'_{XY} , and V'_{ZZ}) is nonuniform, while the second term in the right hand of Eq. (6) vanishes for $\omega = \omega_0$. The effect of the EFG and its inhomogeneity become more significant for the transitions at $\omega_0 \pm \omega_q$ as the magnitude of the quadrupole interaction increases with increasing $|\beta|$. At $\alpha = 0$, $\hbar\omega_q$ [Eq. (4)] is reduced to be $eQ/2 \cdot \{(3 \cos^2 \beta - 1)V'_{ZZ}/2 - \sin^2 \beta V'_{XY}\}$. Assuming that $\Delta V'_{ZZ}$ and $\Delta V'_{XY}$ exists, the fluctuations of V'_{ZZ} and V'_{XY} , the amount of the inhomogeneous broadening by the quadrupole interaction is expressed as

$$\Delta\omega_q = eQ/2 \cdot \{|3 \cos^2 \beta - 1| \Delta V'_{ZZ}/2 + |\sin^2 \beta| \Delta V'_{XY}\}, \quad (7)$$

which monotonously increases with the increase of $|\beta|$ for $0 < |\beta| < 90^\circ$ if $\Delta V'_{XY}$ term is dominant. That condition is expected to be satisfied as the V'_{XY} component has the largest value in the obtained EFG for both ^{75}As and ^{69}Ga . Thus, the β dependence of the NMR line widths shown in Fig. 3(b) suggests that the nonuniformity of the EFG governs the resonance peak broadening at $\omega = \omega_0 - |\omega_q|$ resonance for both ^{75}As and ^{69}Ga . This can be applied to the case of $\omega = \omega_0 + |\omega_q|$. On the other hand, at $\beta = 0$, $\hbar\omega_q$ [Eq. (4)] is reduced to be $eQ/2 \cdot \{(3 \cos^2 \alpha - 1)V'_{ZZ}/2 - \sin^2 \alpha V'_{XY} - \sqrt{2} \sin 2\alpha V'_{XZ}\}$. This also increases with the increase of $|\alpha|$, the same as that of the β dependence. Thus, we consider α dependence of the line widths for $\omega = \omega_0 \pm \omega_q$ is partly affected by the quadrupole interaction in addition to the effective magnetic field by the electron spins.

Besides these interactions, the dipole-dipole interaction should also be taken into account: The nearest-neighbor dipole-dipole interaction is suppressed at the angle configuration ($\alpha = \beta = 0^\circ$) [26]. Because the line width of the $\omega = \omega_0$ resonance is constant with respect to β , however, line width broadening due to the dipole-dipole interaction is negligibly small compared with the hyperfine interaction and the quadrupole interaction.

In conclusion, we have investigated strain and the effects of the quadrupole interaction on nuclear spin states in the n -GaAs (110) QW by the optical TRFR technique. We quantitatively evaluated the EFG of the (110) QW from the dependence of the quadrupolar splitting on the direction of \mathbf{B}_0 and obtained the strain parameters in the QW. Strain plays a key role for spin dynamics in semiconductors so that the quantitative estimation of strain presented in this work enables further understanding of spin-related physics. The fact that the line widths of the NMR spectra change with the direction of \mathbf{B}_0 , suggesting that the NMR line widths are influenced by both the inhomogeneity of the quadrupole interaction and the effective magnetic field by the electron spins, is also explored. These results must be useful for extension of the nuclear spin coherence time as well as to design the quantum structures for future spintronic devices.

This work was partly supported by the Grant-in-Aid for JSPS Fellows and Scientific Research (Grants No. 19048007, No. 19048008, and No. 23246002) from the Ministry of Education, Culture, Sports, Science, and Technology (MEXT), Strategic International Cooperative Program (Joint Research Type), Japan Science and Technology Agency, and the Global COE Program Center of Education and Research for Information Electronics Systems at Tohoku University.

-
- [1] A. Abragam, *The Principles of Nuclear Magnetism* (Oxford University Press, Oxford, 1961).
- [2] V. L. Berkovits and V. I. Safarov, *JETP Lett.* **26**, 256 (1977).
- [3] E. F. Taylor and N. Bloembergen, *Phys. Rev.* **113**, 431 (1959).
- [4] R. K. Sundfors, *Phys. Rev. B* **10**, 4244 (1974).
- [5] W. E. Carlos, S. G. Bishop, and D. J. Treacy, *Phys. Rev. B* **43**, 12512 (1991).
- [6] D. J. Guerrier and R. T. Harley, *Appl. Phys. Lett.* **70**, 1793 (1997).
- [7] H. Knotz, A. W. Holleitner, J. Stephens, R. C. Myers, and D. D. Awschalom, *Appl. Phys. Lett.* **88**, 241918 (2006).
- [8] M. Eickhoff, B. Lenzmann, D. Suter, S. E. Hayes, and A. D. Wieck, *Phys. Rev. B* **67**, 085308 (2003).
- [9] R. I. Dzhirov and V. L. Korenev, *Phys. Rev. Lett.* **99**, 037401 (2007).
- [10] P. Maletinsky, M. Kroner, and A. Imamoglu, *Nature Phys.* **5**, 407 (2009).
- [11] O. Krebs, P. Maletinsky, T. Amand, B. Urbaszek, A. Lemaître, P. Voisin, X. Marie, and A. Imamoglu, *Phys. Rev. Lett.* **104**, 056603 (2010).
- [12] V. K. Kalevich, V. D. Kul'kov, I. A. Merkulov, and V. G. Fleisher, *Sov. Phys. Solid State* **24**, 1195 (1982).
- [13] I.-W. Park, H. Choi, H. J. Kim, H. W. Shin, S. S. Park, and S. H. Choh, *Phys. Rev. B* **65**, 195210 (2002).
- [14] J. M. Kikkawa and D. D. Awschalom, *Science* **287**, 473 (2000).
- [15] G. Salis, D. D. Awschalom, Y. Ohno, and H. Ohno, *Phys. Rev. B* **64**, 195304 (2001).
- [16] M. Poggio, G. M. Steeves, R. C. Myers, Y. Kato, A. C. Gossard, and D. D. Awschalom, *Phys. Rev. Lett.* **91**, 207602 (2003).
- [17] H. Sanada, Y. Kondo, S. Matsuzaka, K. Morita, C. Y. Hu, Y. Ohno, and H. Ohno, *Phys. Rev. Lett.* **96**, 067602 (2006).
- [18] Y. S. Chen, D. Reuter, A. D. Wieck, and G. Bacher, *Phys. Rev. Lett.* **107**, 167601 (2011).
- [19] D. Paget, T. Amand, and J.-P. Korb, *Phys. Rev. B* **77**, 245201 (2008).
- [20] In this experiment, we observed an additional β dependence of the NMR peak frequencies. The data is well fitted by replacing B_0 by $B_0 + B_{\text{eff}}(1 - \cos 2\beta)$. The fitted values of B_{eff} are 0.59 mT for ^{75}As and 0.52 mT for ^{69}Ga . This β dependence agrees qualitatively with the second-order perturbation of the quadrupole Hamiltonian.
- [21] We assumed that the maximum EFG component is positive.
- [22] S. Adachi, *J. Appl. Phys.* **58**, R1 (1985).
- [23] R. H. Henderson and E. Towe, *J. Appl. Phys.* **78**, 2447 (1995).
- [24] D. Sun and E. Towe, *Jpn. J. Appl. Phys.* **33**, 702 (1994).
- [25] M. Ono, H. Kobayashi, S. Matsuzaka, Y. Ohno, and H. Ohno, *Appl. Phys. Lett.* **96**, 071907 (2010).
- [26] M. Kawamura, T. Yamashita, H. Takahashi, S. Masubuchi, Y. Hashimoto, S. Katsumoto, and T. Machida, *Appl. Phys. Lett.* **96**, 032102 (2010).
- [27] T. Ota, G. Yusa, N. Kumada, S. Miyashita, T. Fujisawa, and Y. Hirayama, *Appl. Phys. Lett.* **91**, 193101 (2007).
- [28] *Optical Orientation*, edited by F. Meier and B. P. Zakharchenya (Elsevier, Amsterdam, 1984).